

Theoretical Study of the Mechanisms of Acid-Catalyzed Amide Hydrolysis in Aqueous Solution

Dirk Zahn

Max Planck Institute for Chemical Physics of Solids, Noethnitzer Strasse 40, 01087 Dresden, Germany

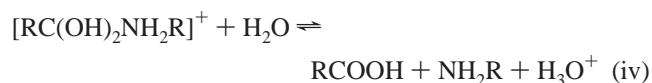
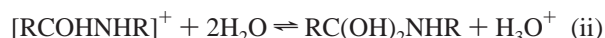
Received: January 22, 2003; In Final Form: July 30, 2003

Acid-catalyzed amide hydrolysis is elucidated by means of Car–Parrinello molecular dynamics simulation. The reaction is investigated in aqueous solution. Therein all molecules, including those of the solvent, are treated quantum mechanically. In our simulations *N*-methylacetamide is taken as a model to describe the amide group of a peptide. The first step in acid-catalyzed amide hydrolysis is the protonation of the carbonyl oxygen atom of the amide group. The rate-determining step is the nucleophilic attack of a water molecule to the carbon atom of the amide group. During this process one proton is transferred to the water phase. In the following, the nitrogen atom of the intermediate is protonated. Finally, the C–N bond is broken, yielding carboxylic acid and methylamine.

Introduction

Amide hydrolysis is a process of great biochemical importance and has been subject to intense investigations in both theory^{1–4} and experiment.^{5–8} At low pH amide hydrolysis occurs via the acid-catalyzed pathway.

This process may be subdivided in four reaction steps.⁸ Step i in acid-catalyzed amide hydrolysis is the protonation of the amide. Though N-protonation was discussed, the protonation of the carbonyl oxygen atom is commonly accepted as the initial step in acid-catalyzed amide hydrolysis.^{8–11} Step ii is the approaching of a water molecule to the carbon atom forming the peptide bond. By emitting one proton, the water molecule is split and a hydroxyl group is added to the carbon atom of the amide. The basic intermediate then absorbs a proton. This occurs via protonation of the amide nitrogen atom. Step iv is the breaking of the C–N bond.



Though this scheme was proposed from experiments already a decade ago,⁸ the mechanism of acid-catalyzed amide hydrolysis could not yet be fully confirmed from theory. This is caused by the difficulty in treating complex reacting systems with sufficient accuracy. So far the ab initio calculations were performed for only a few degrees of freedom. The role of the remaining degrees of freedom was modeled by classical methods. On the basis of such models only the quantum mechanically treated molecules may actually be involved in the reaction. The remaining molecules are considered as passive

solvent and may not react. Thus, by defining the quantum mechanically described subset, one has to take care not to predefine the reaction mechanism.

In reactions discussed here, the water molecules of the solvent may serve as proton donors or acceptors and have to be considered as potential reactants. Those water molecules require a quantum treatment. To be sure of not predefining the reaction pathway, we decided to explore the acid-catalyzed amide bond cleavage in aqueous solution by means of Car–Parrinello molecular dynamics (CPMD) simulations.¹² Therein all electronic degrees of freedom are described quantum mechanically. Thus all molecules are considered as possible reactants.

As a model, *N*-methylacetamide (NMAA) may be chosen to describe a proteins peptide bond. The initial step (i) of acid-catalyzed hydrolysis is the protonation of the amide oxygen atom. For this process the water molecules surely do not act as reactants and may therefore be treated as solvent molecules. NMAA protonation has been elucidated in mixed quantum/classical simulation.¹³ In this paper we investigate the following steps (ii)–(iv) using a full ab initio approach.

Simulation Details

The simulation system includes one molecule of protonized NMAA (HNMAA^+), a chlorine ion, and 31 water molecules in an orthorhombic simulation box of the size $12 \text{ \AA} \times 8 \text{ \AA} \times 8 \text{ \AA}$. The chlorine was introduced as a counterion to achieve charge neutrality. Periodic boundary conditions were applied to mimic an aqueous solution. A suitable initial configuration was obtained at low computational costs by performing classical molecular dynamics (MD) simulations using the DLPOLY package.¹⁴ Therein the time step was chosen as 1 fs. The molecules were treated as rigid and described by an all atoms force field. The parameters for the chlorine were adopted from the optimized potential for liquid simulations (OPLS) force field.^{14,15} All other parameters were taken from a previous study of NMAA protonation.¹³ From 100 ps of NpT simulation at standard conditions the average box volume was determined as 754.56 \AA^3 . Accordingly, the box dimensions were adjusted to $11.79 \text{ \AA} \times 8 \text{ \AA} \times 8 \text{ \AA}$. Then a simulation of 50 ps at constant

* Corresponding author. E-mail: zahn@cfs.mpg.de. Tel: +49 (0) 351 46464205. Fax: +49 (0) 351 46463002.

volume was performed. The final configuration of this run was chosen as the initial system for the CPMD simulations.

The CPMD simulations were carried out within the canonical ensemble. The constant temperature of 300 K was incorporated by a chain of four Nose–Hover thermostats.¹⁶ The orbitals were described by a plane wave basis using an energy cutoff of 70 Ry. The calculations were performed at the Γ point only of the Brillouin zone, and we used norm-conserving pseudopotentials¹⁷ and the BLYP density functional.¹⁸ The choice of basis set and the density functional may significantly affect the accuracy of the quantum calculations. The plane wave cutoff was chosen according to the hardest, i.e., the oxygen pseudopotential. The accuracy of density functionals for the investigation of amide hydrolysis was elucidated by Dobbs and Dixon.¹⁹ Accordingly, the error in reaction energy prediction using the BLYP functional is expected to be around 2 kcal·mol⁻¹. This value was assumed as the error related to the quantum approach in the energy profiles of C–O and C–N bond formation and cleavage, respectively.

To use a larger value as the electronic mass parameter, all hydrogen atoms were replaced by deuterium. In this case a mass parameter of 700 au for the electrons ensures decoupling of the nuclear and the fictitious electronic modes, which is essential to maintain electronic adiabaticity. Consequently, a time step of 0.12 fs was chosen. Because only static properties are investigated, the usage of heavier isotopes of the hydrogen atoms does not affect the simulation results presented in this paper. According to this transferability, we do not alter our writing from hydrogen to deuterium.

Results

To elucidate the nucleophilic attack (ii), the distance of the carbon atom and the oxygen atom of a neighbor water molecule was chosen as a reaction coordinate. The approaching of these atoms is obviously necessary for the formation of a carboxyl group.

We first investigated the reactant state of (ii). From a 5 ps simulation run the closest oxygen–carbon atom distance of a water molecule and the amide group was monitored. The average r_{O-C} distance was found to be 2.63 Å. This was taken as the zero point of the potential of mean force (PMF) profile of the O–C bond formation. The reaction was then investigated in a subsequent series of simulations fixing r_{O-C} to 2.5, 2.25, 2, 1.75, 1.55, and 1.45 Å, respectively. The average constraint force was calculated according to

$$\langle \nabla \text{PMF}(r_{O-C}) \rangle_\tau = - \frac{1}{\tau - \tau_0} \int_{\tau_0}^{\tau} \partial t f_{O-C}(t) dt$$

Here, f_{O-C} is the constraint force at time t and $\tau - \tau_0$ is the sampling period. For each run an equilibration time τ_0 of 1–2 ps was found to be appropriate. The sampling time varied from 2 to 3 ps. As a convergence criterion the fluctuations observed for the last picosecond of the mean force according to the above formulas was demanded to be less than 0.5 kcal·mol⁻¹ Å⁻¹. The product state was monitored from simulation of the free relaxation starting from the run of the last O–C constraint. The related O–C bond length average was found to be 1.47 Å.

An interpolating polynomial was fit to the mean force and the PMF derived from integration. To obtain some estimate for the error related to the fitting procedure, several fits, each omitting one data point, were done. The maximum deviation of the corresponding PMF curves (within the interval 1.45 ≤ r_{O-C} ≤ 2.5 Å) was found to be 0.5 kcal·mol⁻¹. Considering

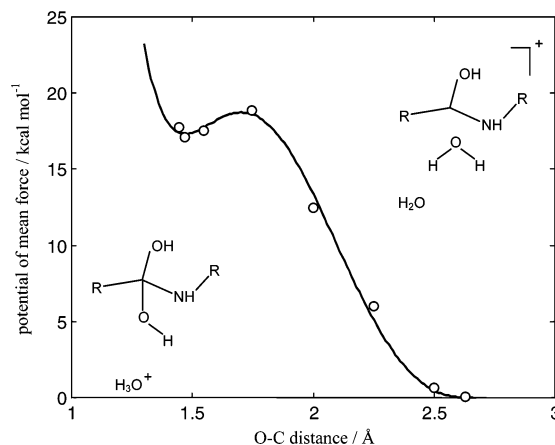


Figure 1. Potential of mean force profile of the nucleophilic attack of the C–N bond as a function of the O–C distance. R = CH₃. The solid line corresponds to the integration of the interpolated constraint force curve, and the circles represent the raw data. Refer to the text for the discussion of the error margins.

the integral of the error in the mean force over an interval of 1 Å and the error estimate related to the quantum approach, the total error margin of the PMF calculations is assumed as 3 kcal·mol⁻¹.

The PMF profile of the nucleophilic attack is shown as a function of the O–C distance in Figure 1. Before discussing the free energy curve quantitatively, this process is investigated from a qualitative point of view.

In the course of the reaction one proton of the water molecule performing the nucleophilic attack is emitted. This proton was found to migrate in the solvent via the Grotthuss type of mechanism, as observed for proton transport in water.^{20–26} On the basis of experimental findings, this mechanism was proposed already a decade ago.⁸ Accordingly, the nucleophilic attack is expected to yield RC(OH)₂NHR and H₃O⁺. This is followed by N-protonation as a separate reaction step.

This is in controversy to the mechanisms predicted from previous theoretical studies of the acid-catalyzed amide hydrolysis.^{1,2} However, in these studies, the solvent water was not explicitly included¹ or at most one extra water molecule was included² in the quantum calculations. Thus the ability of water to solvate the hydronium ion was not considered.

It is noteworthy, that the proton-transfer step is not included in the simple picture of the reaction coordinate considering only the O–C distance. Because of the large number of degrees of freedom, processes in solution may involve reaction coordinates of considerable complexity. A detailed investigation of the reaction coordinate of (ii) based on reaction path sampling is currently in progress. From the presented simulations, only the component of the free energy gradient along the r_{O-C} coordinate may be investigated and the free energy differences according to the proton-transfer step cannot be obtained. However, while the O–C distance is kept fixed, the remaining degrees of freedom were investigated from free dynamics. In the simulation runs with an O–C distance less than 1.7 Å, the proton transfer was observed within a few hundred femtoseconds. Accordingly, once we have installed a small O–C distance, the barrier for the proton transfer may be expected to be around $k_B T$ (≈ 0.6 kcal·mol⁻¹) or less. From this a crude estimate of the upper error margin, related to the choice of the reaction coordinate, in the activation free energy for C–O bond formation may be given as 0.6 kcal·mol⁻¹. However, the effect on the lower error margin may not be assessed in such a simple way.

Different is the situation for the calculation of the PMF difference of reactant and product state. The gain in free energy resulting from the proton transfer cannot be estimated in this simple way. Accordingly, only the activation free energy of C–O bond formation is expected to be, within the discussed error margin, a quantitative result. The free energy for the back-reaction cannot be obtained from the presented simulations.

At an O–C distance of 1.7 Å the PMF profile exhibits a barrier of about 19 ± 3 kcal·mol⁻¹. The acid-catalyzed hydrolysis of *N*-methylacetamide was investigated experimentally by Bolton and co-workers.^{27,28} In these studies the activation free energy was found as 21.5 ± 0.3 kcal·mol⁻¹. Accordingly, the CPMD simulations are, within the discussed error margins, found to be in nice agreement with the experiment.

In the course of the nucleophilic attack, the amide's character changes from acidic to basic. This may be seen from the distribution of the distances between the nitrogen atom and the hydrogen atoms. In average, the closest N–H distance changes from 2.75 Å in the reactant state to 1.76 Å in the product state. Though the formation of a strong hydrogen bond may be observed, the nitrogen atom is not protonated during this reaction step. Thus N-protonation has to be considered as a separate reaction step. The excess proton is preferably migrated in the water phase.

The protonation of the nitrogen atom of H₃C₂(OH)₂NHCH₃ may occur via two different pathways. The first one involves proton transfer from a hydronium ion. However, a proton may also be absorbed from a water molecule, yielding H₃C₂(OH)₂NH₂CH₃⁺ and OH⁻.

The N-protonation by an excess proton in the water phase could be observed from direct molecular dynamics simulation. Thus, the activation free energy is expected to be small in comparison to $k_B T$ or the process is even activationless. The rate-limiting part of this reaction step is the diffusion of the excess proton to the first solvent shell of the nitrogen atom of the amide.

To complete the picture of reaction step iii, N-protonation by an adjacent water molecule is elucidated. As a reaction coordinate, the distance of the amide nitrogen atom and a proton of a neighbor water molecule is chosen. In the initial state, the average N–H distance is around 1.8 Å. Again, this was taken as the zero point of the potential of mean force (PMF) profile of the reaction. The nitrogen protonation is then induced by constraining the N–H distance to 1.7, 1.5, 1.3, and 1.2 Å. After 1–2 ps equilibration, the average constraint force was computed from 3 to 5 ps simulations. The product state of the reaction was found to be metastable and can be observed in absence of constraints. After imposing N-protonation by constraining the N–H distance to 1.1 Å, the dynamics of the free system was simulated. From this trajectory, the PMF profile in the product region was calculated from the probability distribution of the N–H bond length. Figure 2 shows the potential of mean force (PMF) as a function of the N–H distance. The protonation of the amide nitrogen atom by an adjacent water molecule is related to a barrier of 5 ± 3 kcal·mol⁻¹.

We expect N-protonation to occur mainly by excess protons from the water phase. The ratio of the two competing pathways is surely related to proton concentration in the solvent. However, in the course of step ii an excess proton is produced. Though solvated in the water phase, this proton is located in the proximity of the amide, which may enhance N-protonation via proton diffusion.

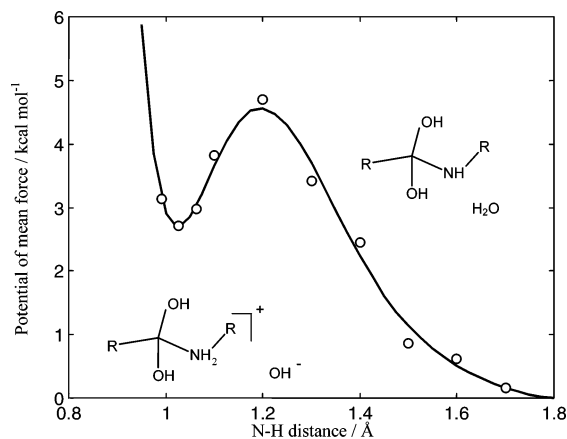


Figure 2. Potential of mean force profile of N-protonation by an adjacent water molecule. The solid line corresponds to the integration of the interpolated constraint force curve, and the circles represent the raw data. Refer to the text for the discussion of the error margins.

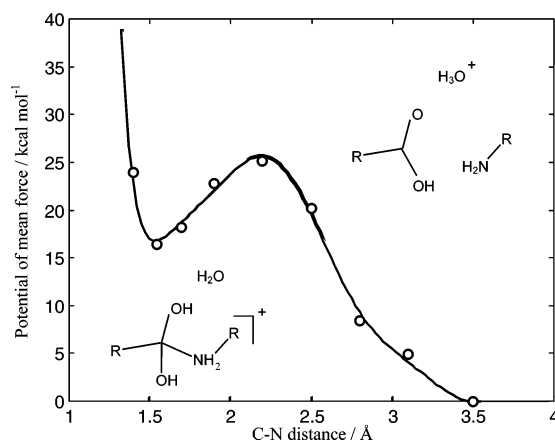


Figure 3. Potential of mean force profile of C–N bond dissociation of the H₃C₂(OH)₂NH₂CH₃⁺ intermediate. The solid line corresponds to the integration of the interpolated constraint force curve, and the circles represent the raw data. Refer to the text for the discussion of the error margins.

The last step of the hydrolysis is the breaking of the C–N bond (iv). This process was investigated by taking the C–N distance as the reaction coordinate. In H₃C₂(OH)₂NH₂CH₃⁺ the C–N bond length varies around 1.54 Å. To induce the bond breaking, r_{C-N} was fixed to 1.7, 1.9, 2.2, 2.5, 2.8, 3.1, and 3.5 Å. At 3.5 Å the average constraint force was found to be around zero. This was taken as the product state of the C–N bond cleavage. The PMF profile for reaction step iv is illustrated in Figure 3. The transition state is located at a C–N distance of 2.3 Å, related to an activation free energy of 9 ± 3 kcal·mol⁻¹. The breaking of the C–N bond is accompanied by deprotonation of one of the hydroxyl groups. This proton-transfer step is not included in the simple picture of assuming the C–N bond length as the reaction coordinate for H₃C₂(OH)₂NH₂CH₃⁺ dissociation. Analogous to the discussion of reaction step ii an additional error in the activation free energy is estimated as 0.6 kcal·mol⁻¹. Within the given accuracy, the difference in free energy barriers of steps ii and iv clearly shows the nucleophilic attack to be the rate-determining one.

It is interesting to observe the fate of the proton emitted from H₃C₂(OH)₂NH₂CH₃⁺ during C–N bond breaking. In the gas phase, this proton is transferred to the amide, yielding CH₃COOH and NH₃CH₃⁺.¹ However, in aqueous solution the excess proton is migrated in the water phase.

From experiment, the breaking of the C–N was found to involve a concerted proton transfer from one OH group to an adjacent water molecule.^{7,8} Thus, as for reaction step ii the mechanism, as observed from simulation, of (iv) is in agreement with experimental findings. This also applies to the finding of the nucleophilic attack rather than the C–N bond cleavage being the rate-determining step.

Conclusion

We presented CPMD simulations of the acid-catalyzed amide hydrolysis in aqueous solution. Therein an explicit solvent model is used and all molecules are treated quantum mechanically. NMAA is used as a model for the amide group of a peptide. The reaction was induced by imposing distance constraints. From our simulations, free energy profiles are derived from integration of the constraint forces and from PMF calculations of unconstrained trajectories.

The reaction occurs as a four-step process. The initial step is the protonation of the carbonyl oxygen atom of the amide. The second and rate-determining step is the nucleophilic attack of a water molecule to the carbon atom of the amide group. During this process one proton is transferred to the water phase. This is followed by the protonation of the intermediate nitrogen atom in a separate reaction step. Both protonation by a hydronium ion and by dissociation of a water molecule are elucidated. Finally, the dissociation of the C–N bond is investigated. During this process one proton is emitted to the water phase, yielding CH₃COOH, NH₂CH₃, and H₃O⁺.

Acknowledgment. I thank Michele Parrinello for generously supporting this work.

References and Notes

(1) Krug, J. P.; Popelier, P. L. A.; Bader, R. F. W. *J. Phys. Chem.* **1992**, *96*, 7604–7616.

- (2) Antonczak, S.; Ruiz-Lopez, M. F.; Rivail, J. L. *J. Am. Chem. Soc.* **1994**, *116*, 3912–3921.
- (3) Stanton, R. V.; Peräkylä, M.; Bakowies, D.; Kollman, P. A. *J. Am. Chem. Soc.* **1998**, *120*, 3448–3457.
- (4) Bakowies, D.; Kollman, P. A. *J. Am. Chem. Soc.* **1999**, *121*, 5712–5726.
- (5) Hine, J.; King, R. S.-M.; Midden, W. R.; Sinha, A. *J. Org. Chem.* **1981**, *46*, 3186–3189.
- (6) Robinson, B. A.; Tester, J. W. *Int. J. Chem. Kinet.* **1990**, *22*, 431–448.
- (7) Slebocka-Tilk, H.; Bennet, A. J.; Hogg, H. J.; Brown, R. S. *J. Am. Chem. Soc.* **1991**, *113*, 1288–1294.
- (8) Brown, R. S.; Bennet, A. J.; Slebocka-Tilk, H. *Acc. Chem. Res.* **1992**, *25*, 481–488.
- (9) O'Connor, C. *Q. Rev. Chem. Soc.* **1970**, *24*, 553–564.
- (10) Smith, C. R.; Yates, K. *Can. J. Chem.* **1972**, *50*, 771–773.
- (11) Kresge, A. J.; Fitzgerald, P. H.; Chiang, Y. *J. Am. Chem. Soc.* **1973**, *96*, 4698–4699.
- (12) CPMD, Hutter, J.; Alavi, A.; Deutsch, T.; Bernasconi, M.; Goedecker, S.; Marx, D.; Tuckerman, M.; Parrinello, M. MPI für Festkörperforschung und IBM Zürich Research Laboratory, 1995–1999.
- (13) Zahn, D.; Schmidt, K. F.; Kast, S. M.; Brickmann, J. *J. Phys. Chem. A* **2002**, *106*, 7807–7812.
- (14) Smith, W.; Forester, T. *J. Mol. Graph.* **1996**, *14*, 136.
- (15) Jorgensen, W. L. *J. Am. Chem. Soc.* **1996**, *118*, 11225.
- (16) Martyna, G. J.; Klein, M. L.; Tuckerman, M. E. *J. Chem. Phys.* **1992**, *97*, 2635.
- (17) Trolhier, N.; Martius, J. *Phys. Rev. B* **1991**, *43*, 1993.
- (18) Becke, A. D. *Phys. Rev. A* **1988**, *38*, 3098. Lee, C. L.; Yang, W.; Parr, R. G. *Phys. Rev. B* **1988**, *37*, 785.
- (19) Dobbs, K. D.; Dixon, D. A. *J. Phys. Chem.* **1996**, *100*, 3965.
- (20) Tuckerman, M.; Laasonen, K.; Sprik, M.; Parrinello, M. *J. Phys. Chem.* **1995**, *99*, 5749.
- (21) Tuckerman, M.; Laasonen, K.; Sprik, M.; Parrinello, M. *J. Chem. Phys.* **1995**, *103*, 150.
- (22) Marx, D.; Tuckerman, M.; Hutter, J.; Parrinello, M. *Nature* **1999**, *397*, 601.
- (23) Lobaugh J.; Voth, G. A. *J. Chem. Phys.* **1996**, *104*, 2056 and references therein.
- (24) Vuilleumier, R.; Borgis, D. *J. Phys. Chem. B* **1998**, *102*, 4261.
- (25) Zahn, D.; Brickmann, J. *Isr. J. Chem.* **1999**, *39*, 483.
- (26) Agmon, N. *Isr. J. Chem.* **1999**, *39*, 493.
- (27) Bolton, P. D. *Aust. J. Chem.* **1966**, *19*, 1013.
- (28) Bolton, P. D.; Jackson, G. L. *Aust. J. Chem.* **1971**, *24*, 969.